Unsupervised Perception-based Image Restoration of Semi-transparent Degradation using Lie Group Transformations

V. Bruni, E. Rossi, D. Vitulano
Dept. SBAI University of Roma Sapienza, Via A. Scarpa 16,00161 Rome, Italy
Istituto per le Applicazioni del Calcolo, C.N.R., Via dei Taurini 19, 00185 Rome, Italy
bruni@dmmm.uniroma1.it {e.rossi,d.vitulano}@iac.cnr.it

ABSTRACT

This paper presents a generalized model for the removal of semi-transparent defects from images of historical or artistic value. Its main feature is the combination of Lie group transformations with human perception rules that makes restoration more flexible and adaptive to defects having different physical or mechanical causes. Specifically, Lie groups allow to define a redundant set of transformations from which it is possible to automatically select the ones that better invert the physical formation of the defect. Hence, the restoration process consists of an iterative procedure whose main goal is to reduce defect visual perception. The proposed restoration method has been successfully tested on original movies and photographs, affected by line-scratches and semi-transparent blotches.

Keywords: Image Restoration, Lie Groups, Human Visual System, Semi-transparent Defects.

1 INTRODUCTION

In the last years, there has been an increasing demand for the fruition of archived material thanks to the growing development of digital devices. Hence, a lot of research effort has been devoted to propose novel and adaptive digital restoration methods able to deal with image defects like noise, line-scratches, tear, moire, blotches, shake and flicker — see [1]-[12]. If on the one hand, the variety of degradations has led to the definition of specific detection and restoration models in order to guarantee a better precision and adaptivity to different scenarios; on the other hand, the advent of new devices and the up-to-date digital technology has led to the need of a general framework able to simultaneously and globally manage different kinds of degradation. This entails the definition of a new restoration paradigm that puts human eye as the final image consumer and judge, independently of the specific processing method. That is why human perception is gaining a significant role in image processing techniques [13]-[16]. In this perspective, the main goal of digital restoration must be the perceived quality of the restored images. In [17] the authors tried to formalize a global detection/restoration framework based on both physical and visual characteristics of the class of analysed defects. It was mainly based on the following observation. Image defects are detected by human eye 'at first glance' even in complicated contexts as they represent 'anomalies' in natural images. Hence, the reduction of the visual contrast of the degraded region (visual anomaly) should decrease the visual contribution of the degraded area without creating new artifacts. The model basically simulates the Human Visual System (HVS) response to the presence of the defect by projecting the degraded image J into a new space where the defect becomes the most visible object of the scene. This space depends on both the physical cause of the defect and the resolution at which the defect shows its greatest visibility and it allows to define appropriate and automatic detection and restoration operators. They still depend on the physical cause of the defect that, in turn, gives the 'a priori' information that makes the restoration process somewhat independent of the specific image. The deeper the knowledge about degradation, the lower the dependence of restoration on the original image.

However, it is not always possible to have detailed information about the degradation under exam. Moreover, though their different original causes, many defects can show the same features on the image, such as color, shape, etc.. For example, water blotches or foxing often have the same visual appearance on the image, as well as cracks and scratches, or yellowing and fading. Anyway, independently of their different nature, these defects preserve the perception at first sight as common and primary feature.

The main goal of this paper is then the definition of a general restoration framework that aims at being almost independent of a priori specific assumptions on the degradation under exam. The framework is required to select suitable transformations from a redundant set only accounting for reduced 'a priori' information about the defect under exam, as, for example, the semi-transparency of the degraded region. In this way, the same restoration algorithm can be used for a very wide class of image degradations. This kind of framework could really be of interest in several applications since it promotes and facilitates its use by non expert people and, at the same time, it avoids the development of integrated softwares able to deal with specific kinds of degradation. To this aim the role of HVS has to be emphasized in the whole restoration process by introducing proper mathematical concepts and tools. This paper represents a first contribution to this challenging purpose. It will use Lie groups theory combined with HVS rules for defining continuos transformations that also include the ones that better correlate with the degradation process. In fact, a local contrast-based restoration process that embeds transformations in a Lie group gives us the opportunity of defining a redundant set of transformations that also contains the inversion of the unknown degradation process. Furthermore, it allows to develop a restoration algorithm that automatically selects the more suitable transformations for points having the same visual contrast. In fact, infinitesimal operations in Lie algebras and their integration in global transform in Lie groups are able to model some human visual phenomena, as deeply investigated in [18] and [19]. In this paper Lie groups are of great importance since the final solution (original not degraded image) is not known in advance as well as the exact degraded process. The only assumption is the knowledge of the degradation map. However, the flexibility of the proposed model allows this map to be not precise as it will be discussed later. Hence, the proposed model has the following advantages: *i)* the combination of HVS and Lie algebra allows the restoration model to have not a precise target to converge. The model is only required to force the contrast of the final solution to be in a suitable range of values according to typical contrasts of the surrounding clean image — degradation has to be invisible. *ii)* the variability of Lie group transformations and their combination allows a more flexible model for the degraded image — they also include the simpler and widely used translation and shrinking operations [9, 4, 2].

The remainder of the paper is the following. Next section gives a brief review of Lie Algebra and Lie group transformations. Section 3 presents the proposed restoration methodology and its refinement for two kinds of semi-transparent defects: line-scratches and blotches. Finally, Section 4 presents some experimental results and concluding remarks.

2 LIE ALGEBRAS AND LIE GROUPS TRANSFORMATIONS

In the following, we give few mathematical details about Lie algebra and groups useful to understand the proposed approach. For a complete treatment of this topic see, for instance, [20] and [21].

A finite Lie group G is both a multiplicative group and a differentiable manifold, that is G is a group locally diffeomorphic to R^n, if n is its dimension. As a result, a Lie group G has got both algebraic and geometric properties, thanks to the group structure and the differentiable structure respectively, and they are deeply related. Finally, every Lie group of finite dimension can always be viewed as a matrix group.

Since a Lie group is a manifold, it has a tangent space at the identity element e, called its Lie algebra, namely $\mathfrak{g}$, which is a vector space of the same dimension of G. The exponential map $\exp : \mathfrak{g} \to G$ gives a natural way to move from the Lie algebra $\mathfrak{g}$ (vector space) to the group G (manifold) and, in the case of finite matrix group, it has a very simple form since it corresponds to matrix exponential: if $X \in \mathfrak{g}$, i.e. X is a tangent vector at e in G, then $\exp(X) = \sum_{n=0}^{\infty} \frac{X^n}{n!}$.

Most of the matrix Lie groups can be used to describe transformations in the plane or in the space. The dimension of the group is the number of free parameters needed to describe the transformations; its Lie algebra elements are tangent vectors at the identity and represent infinitesimal transformations of the points. In this paper we are interested in projective transformations that can be described as a group matrix, P_n, acting on points of $\mathbf{R}^n$ expressed in homogeneous coordinates, with the convention that the $(n+1)-$th value in the coordinates is always scaled back to 1. Projective transformations are characterized by $m = n(n+2)$ parameters (dimension of P_n), described by the elements $G_1, G_2, \ldots, G_m$ of a Lie algebra basis. For instance, for $n = 2$

$$G_1 = \begin{pmatrix} 0 & 0 & 1 \\ 0 & 0 & 0 \\ 0 & 0 & 0 \end{pmatrix} \quad G_2 = \begin{pmatrix} 0 & 0 & 0 \\ 0 & 0 & 1 \\ 0 & 0 & 0 \end{pmatrix} \qquad \textit{translations}$$

$$G_3 = \begin{pmatrix} 1 & 0 & 0 \\ 0 & 0 & 0 \\ 0 & 0 & 0 \end{pmatrix} \quad G_4 = \begin{pmatrix} 0 & 0 & 0 \\ 0 & 1 & 0 \\ 0 & 0 & 0 \end{pmatrix} \qquad \textit{scaling}$$

$$G_5 = \begin{pmatrix} 1 & 0 & 0 \\ 0 & -1 & 0 \\ 0 & 0 & 0 \end{pmatrix} \textit{rotation} \quad G_6 = \begin{pmatrix} 0 & 1 & 0 \\ 1 & 0 & 0 \\ 0 & 0 & 0 \end{pmatrix} \textit{shear}$$

$$G_7 = \begin{pmatrix} 0&0&0 \\ 0&0&0 \\ 1&0&0 \end{pmatrix} \quad G_8 = \begin{pmatrix} 0&0&0 \\ 0&0&0 \\ 0&1&0 \end{pmatrix} \quad \textit{projections.}$$

Hence, every real linear combination of $G_1, ..., G_m$ is an infinitesimal projective transformation in the vector space that corresponds to a transformation of the group P_n thanks to the exponential map. The infinitesimal transformation of a generic point $p \in \mathbf{R}^n$ is $\tilde{L}_j = G_j \tilde{p}$, where $\tilde{p}$ is the point p expressed in homogeneous coordinates. We denote by L_j the corresponding affine coordinates of $\tilde{L}_j, \quad j = 1, \ldots, m$. Hence, for $n = 2$, we have

$$L_1 = \begin{pmatrix} 1 \\ 0 \end{pmatrix} \quad L_2 = \begin{pmatrix} 0 \\ 1 \end{pmatrix} \quad L_3 = \begin{pmatrix} x \\ y \end{pmatrix} \quad L_4 = \begin{pmatrix} x \\ -y \end{pmatrix}$$

$$L_5 = \begin{pmatrix} y \\ -x \end{pmatrix} \; L_6 = \begin{pmatrix} y \\ x \end{pmatrix} \; L_7 = \begin{pmatrix} xy \\ y^2 \end{pmatrix} \; L_8 = \begin{pmatrix} x^2 \\ xy \end{pmatrix}.$$

3 THE PROPOSED RESTORATION MODEL

The degraded image J at the point $p = (x, y)^T$ can be modeled as

$$J(p) = \mathcal{T}(I(p)),$$

where $\mathcal{T}$ is the unknown degradation transformation and I is the original image. The goal should be to find the inverse of $\mathcal{T}$, namely $\mathcal{T}^{-1}$, in order to reconstruct the original image I. The key point is that $\mathcal{T}$ is unknown. The proposed model set a suitable group of eventually redundant transformations where automatically select $\mathcal{T}^{-1}$. In particular, the selected group is the group of projective transformations (in the plane or in the space as we will explain later): it contains translation and shrinking operations commonly used in restoration models but also rotations, shears and projections. Hence, we fix a group of transformations and the iterative procedure that selects their best composition, rather than a specific type of transformation. Moreover the projective group is a Lie group and its geometrical structure is exploited in order to define a simple iterative procedure to select $\mathcal{T}^{-1}$.

3.1 Distance minimization

The iterative procedure presented in [22] has been used. It mainly exploits the relation between Lie algebras and Lie groups to map a given submanifold S_1 of $\mathbb{R}^n$ to another one, S_2, through a suitable composition of transformations of the group, minimizing their distance. More precisely, let $p \in S_1$, n_p the unit normal at S_1 in p and d_p the distance between p and S_2 along n_p. So $d = \sum_{p \in S_1} d_p$ is the global distance between S_1 and S_2. The Lie group structure allows to look for an infinitesimal transformation inside the Lie algebra (that is a vector space), instead of a global transformation of the group, and then to move it to the group by the exponential map. So the problem is linear and the goal is just to find $\alpha_1, ..., \alpha_m \in \mathbb{R}$, such that the corresponding infinitesimal action on p, that is $\sum_{j=1}^m \alpha_j L_j^p$, projected onto the normal direction n_p minimizes d, that is

$$(\alpha_1, \ldots, \alpha_m) =$$
$$= arg \min_{\alpha_j} \sum_{p \in S_1} \left(d_p - \sum_{j=1}^m \alpha_j \left(L_j^p \cdot n_p \right) \right)^2 . \quad (1)$$

Therefore, $\vec{\alpha} = (\alpha_1 \ldots \alpha_m)^T$ is such that $\vec{\alpha} = \vec{A}^{-1} \vec{b}$, where $\vec{A}$ is the matrix whose elements A_{jh} are defined as follows

$$A_{jh} = \sum_{p \in S_1} \left(L_j^p \cdot n_p \right) \left(L_h^p \cdot n_p \right)$$

while $\vec{b}$ is a column vector whose elements are

$$b_h = \sum_{p \in S_1} d_p \left(L_h^p \cdot n_p \right).$$

Hence, $t = \sum_{j=1}^m \alpha_j G_j$ is the infinitesimal transformation in the Lie algebra that minimizes the distance between S_1 and S_2 and $T = \exp(t)$ its corresponding element in the group. S_1 is updated applying T to its points and the minimization algorithm is applied to the new couple $\left(S_1^{(1)}, S_2 \right)$,where $S_1^{(1)} = T(S_1)$, and so on until the distance between S_1 and S_2 is small enough. For the numerical computation of $\exp(t)$ applied to generic point p, a 4th order Runge Kutta algorithm can be used — see [22] for details. It is equivalent to cut the 4th order series expansion of the matrix exponential and apply it to the point p, that is

$$T \approx I + t + \frac{1}{2} t^2 + \frac{1}{6} t^3 + \frac{1}{24} t^4,$$

but it directly manages affine coordinates.

It is worth stressing that this procedure has much in common with the basic concepts of convex projections for restoration, described in [23]. However, in this case we do not use neither convex sets nor orthogonal projections, but only iterated projective transformations in $\mathbb{R}^n$ and their algebraic and geometrical properties.

3.2 HVS embedded in the minimization algorithm

We would like to apply the iterative procedure described in the previous section to the damaged image by modeling it as a suitable submanifold S_1 of $\mathbb{R}^n$, in order to select the transformations that move S_1 towards the clean image S_2. It is worth observing that for blotches restoration, $n = 3$ and

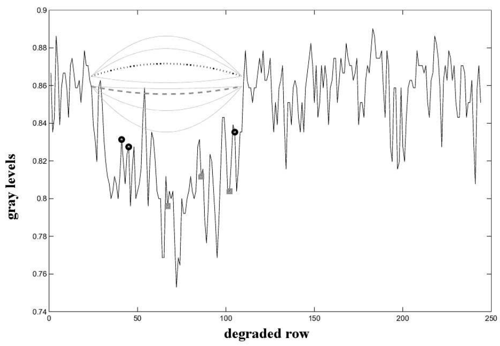

Figure 1: Parabolas are the target curves used in the iterative procedure. Markers are in correspondence to two different groups of points selected with the SMQT transform. Dashed and dotted parabolas are their corresponding target curves.

the whole degraded area is modeled as a surface in $\mathbb{R}^3$ while for scratch restoration $n = 2$ and each degraded row is modeled as a curve in $\mathbb{R}^2$. Unfortunately, in case of digital restoration the final clean image is unknown so that the aforementioned procedure would be unfeasible.

To take advantage of the aforementioned method and to preserve the original image information, HVS perception mechanisms can be embedded in the restoration process. They allow us to define a suitable range of admissible intensity values for the damaged area to be not visible with respect to its neighborhood. In other words, to be invisible, the degraded region must be contained in a certain **cone of visibility**, that depends on the global intensity value of the analysed image; at the same time, abrupt changes in the final solution are not allowed in order to avoid artifacts in correspondence to the frontier of the degraded region. The range of admissible values for the final solution cannot exceed the one of the surrounding information, in terms of visibility bounds, in order to be perceived as a natural scene component. The **cone of visibility** for $n = 2$ can be then defined as in Fig. 1, where the upper and lower parabola curves respectively reach the greatest and least allowed values, namely r_2 and r_1, and the initial point of the **cone of visibility** is in the range of invisible luminance value with respect to the average of the surrounding information [25]. To obtain it, the visual contrast of pixels in the area around the initial points, namely R, must satisfy Weber's law, i.e. $\frac{I_R - I_B}{I_R} < \tau$, where I_R and I_B are the luminance of the region R and its background B, while τ is the just noticeable threshold [24]. For $n = 3$, the cone is defined in the same way replacing parabolas with paraboloids. The cone of visibility is then the target S_2. Hence, the degraded image is moved inside the cone by the distance minimization iterative procedure in order to make the damage invisible.

However, a further consideration has to be made for semi-transparent degradation. Despite the wide flexibility of Lie transformations, the minimization process in eq. (1) is global. In fact, at each step the parameters $\{\alpha_j\}_{j=1,\dots,m}$ are the same for each point of the degraded area. Hence, if on the one hand global transformations preserve the original information contained in the degraded region, on the other hand they forget that pixels may have been subjected to a different amount of degradation. In order to find a tradeoff between preservation of original information and model flexibility, it is necessary to classify damaged pixels accounting for their visual feature and restore them accordingly. We aim at processing in the same way points that are equally perceived by human eye i.e., points having the same visual contrast have to converge to the same target sub-manifold. In order to classify pixels with the same visual contrast, the Successive Mean Quantization Transform (SMQT) [26] is used. It groups pixels having the same visual features. More precisely SMQT builds a binary tree using the following rule: given a set of data D and a real parameter L (number of levels), split D into two subsets, $D_0 = \{x \in D | D(x) \leq \overline{D}\}$ and $D_1 = \{x \in D | D(x) > \overline{D}\}$, where $\overline{D}$ is the mean value of D. D_0 and D_1 are the first level of the SMQT. The same procedure is recursively applied to D_0 and D_1 and so on until the L^{th} level, that is composed by 2^L subsets. Each group belongs to a sub-manifold (defined by interpolation). The target sub-manifold of the i-th group is defined as a paraboloid (parabola) cut by the plane $z = M + \Delta$ (line $y = M + \Delta$) for $n = 3$ ($n = 2$), where M is the mean value of the intensity surrounding values and Δ accounts for the global visibility of the degraded area with respect to the external one, and whose vertex is proportional to the mean value of the group. Hence, each group converges to the corresponding sub-manifold, as shown in Fig. 1, according to the minimization in eq. (1). The iterative minimization process stops when the target sub-manifold has been reached, in agreement with visibility bounds. More precisely, if $S_1^{(K)}$ is the solution at the K-th iteration for the $i-$th group and S_2 the corresponding target sub-manifold, then $S_1^{(K)}$ is an acceptable solution if

$$\frac{\sum_p |S_1^{(K)}(p) - S_2(p)|}{\sum_p S_2(p)} \leq \tau \, , \tag{2}$$

where the first member is the Weber's contrast [24, 27] evaluated at the points of the analysed submanifolds, while τ is the just noticeable detection threshold for that visual contrast [24, 27].

Summing up, HVS is exploited for 1) classifying groups of pixels according to their visual contrast; 2) defining the cone of visibility and the target submanifolds inside it that have to be reached by each group of pixels; 3) defining the stopping criteria for the iterative procedure.

In the next sub-section the whole restoration algorithm is presented. Afterward, two well known semi-transparent defects are briefly presented: line scratches and blotches. They represent an interesting case study. In fact, the physical formation of semi-transparent defects can be complex and can depend on several conditions and events that cannot be known or reproduced in real applications. They can be caused by dirt or moisture on archived material as well as mechanical stress of the support. Hence, they often partially obscure image regions (see Fig. 2) and appear as more or less irregular regions with variable shape and size, having a slightly different color from the original one [7, 9]. They can be then easily confused with scene components since they do not completely hide the underlying original information, that must be retained (after restoration) for its historical and/or artistic value.

3.3 The Algorithm

In the following, the whole restoration algorithm is briefly summarized.

1. Estimate the extrema of the **cone of visibility** r_1, r_2 from the surrounding information. They respectively are the minimum and maximum values of a neighborhood of the degraded area;
2. Apply SMQT to the degraded area;
3. Compute the target curves whose vertices are set according to the mean amplitudes of the groups computed in step 2 and the output of step 1;
4. For each group in step 2, apply the iterative procedure in Section 3.2, where the targets are the ones of step 3, until eq. (2) is satisfied;
5. Perform masking refinement.

The last step is different according to the degradation kind. For semitransparent blotches it corresponds to the study of the contrast properties of pixels in order to understand if degraded pixel are already masked by the original image; for line-scratches it corresponds to apply the visibility-based weights in eq. (5), as next section shows.

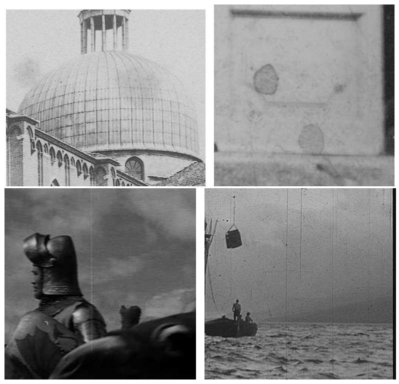

Figure 2: Examples of semi-transparent defects in real photographs and movies.

3.4 Line scratches

Line scratches are common defects on old film sequences. They appear as straight lines spreading over much of the vertical extent of an image frame, as shown in Fig. 2. They can have a different color and are of a limited width [7]. They are often caused by mechanical stress during the projection of a film and occupy the same or a similar location in subsequent frames. The works [1] and [28] provided a physical model for the observed scratches. It has been proved that they are the result of light diffraction effect that occurs during the projection and/or the scanning process. In fact, a scratch is a thin slit on the film material and it is crossed by the light in the projection process. Since the slit (width and depth) is not uniform as a different amount of the original information is removed in the degradation process, the damaged area can be modeled as a partially missing data region and it is well represented by the following equation

$$J(x,y) = (1-(1-\gamma)e^{\frac{-2}{\omega_p}|y-c_p|})I(x,y)+(1-\gamma)L_x(y) \quad (3)$$

where (x, y) are the coordinates of image pixels, $L_x(y)$ is the 1D function model for the scratch, i.e.

$$L_x(y) = b_p sinc^2\left(\frac{y-c_p}{\omega_p}\right), \quad (4)$$

with b_p, c_p and ω_p respectively the maximum brightness, the location (column number) and the horizontal width of the scratch on the image. γ is a normalization parameter that measures the global visibility of the scratch in the degraded image, while $e^{\frac{-2}{\omega_p}|y-c_p|}$ approximates the positive decay of the scratch contribution from its central part toward its end. γ compares the average energy of the peaks of the horizontal cross-section of the image with the one of the scratch and it is in the range $[0, 1]$; hence, the smaller γ the more perceptible the scratch.

Taking into account the reduced horizontal width of a line-scratch, n is set equal to 2, the minimization algorithm is applied row by row and the limiting curves of the **cone of visibility**, as in Fig. 1, are the ones to which the iterative procedure has to converge. However, accounting for the impulsive nature of the defect, as in the equation model (4), a refinement of the final solution is required, according to the scratch visibility with respect to its local context. More precisely, for each point of the scratched area the following weight is applied to the output of the minimization process in eq. (1)

$$\bar{S}_1^{(K)}(x, y) = w(y) S_1^{(K)}(x, y), \tag{5}$$

where $w(y) = \gamma e^{\frac{-2}{\omega_p}|y - c_p|}$, according to the degradation model in eq. (3).

3.5 Semi-transparent blotches

Such blotches are caused by water penetration into paper or chemical reactions whose final visual effect is a darker region on the document with variable shape, color and intensity. Unfortunately, the lack of distinctive features, like shape and color, does not allow the definition of a precise model for the degraded image. However, part of the original information still survives after the degradation process. Due to the larger physical dimension of the blotch with respect to the line scratch, n is set equal to 3 and the distance minimization algorithm is applied to the whole degraded area modeled as a surface in $\mathbf{R}^3$. The group of projective transformations in the space has dimension 15 and it contains the same types of transformations as for $n = 2$. The restoration process is exactly the one described above. Anyway, due to the high semi-transparency of this kind of defects and its variable dimension, a different amplitude of the cone of visibility has to be used for the darkest and brightest points of the degraded area. Hence, a pre-processing step to separate darkest and brightest region of the damage is required. Moreover, in the masking refinement, the study of contrast properties allows to understand if pixels are already masked by original image information: in this case it may be more convenient to leave them unchanged to avoid the creation of annoying artifacts, as it is described in detail in [29].

4 EXPERIMENTAL RESULTS

The proposed approach has been tested on selected images from the photographic Alinari Archive in Florence, affected by semi-transparent defects and on several real sequences (digitized copies of actual damaged films) having different subjects and of 1-2 minutes length (1500- 3000 frames). Some results are shown in Figs. 3 and 4. It is important to test the method on real damages. Since the precise physical process and the corresponding real transformation are unknown, artificial defects are not representative of real applications on archived material.

In all tests, the size of the neighbouring area of the degraded region is three times the one of the degraded area, while the number of groups of the SMQT in step 2 has been set equal to 8 for semi-transparent blotches and 2 for line scratches. The visual quality of the restored images is very satisfactory. Textures are well preserved as well as details of the original image information, while annoying artifacts, like spikes, halo effects or over-smoothed regions, do not appear. In fact, the different processing of pixels having different contrast value contributes to the flexibility of the restoration model. The convergence process is different for each group of points so that it could happen that some groups converge after one or two iterations while others require longer convergence time. In that way, the restoration process has two main advantages: halo effects at the borders of the degraded region and over-smoothing of the restored pixels are missing. In addition, the refinement procedure allows to successfully deal with some delicate cases, as the intersection between the degraded area and a darker region of the image as the third example in Fig. 3 and the Knight shoulder in Fig. 4, and also to make the restoration process more independent of detection results. Finally, it is worth emphasizing two additional advantages of the proposed method. Even though it involves iterative procedures to converge to the final solution, it uses simple and fast operations so that just 4/5 iterations on average are required for convergence. The time of each iteration depends on both the dimensions of the image and the degraded area. For instance, in the case of the blotch in Fig. 5, each iteration takes 45 seconds on average; in the case of the scratch in Fig. 6, each iteration for each row takes just 1/2 seconds. In addition, the algorithm does not require user's interaction, since it automatically adapts each of its steps to the analyzed image.

For the sake of completeness, the restoration results have been compared with some recent restoration methods of semi-transparent defects [9, 4, 2, 28]. Since the clean image is not available in real applications, quantitative measures or metrics to determine the goodness of the restoration are not convenient. Comparison is then based on the perceived visual quality: some results are shown in Figs. 5 and 6. As it can be observed, the proposed restoration procedure gives high quality im-

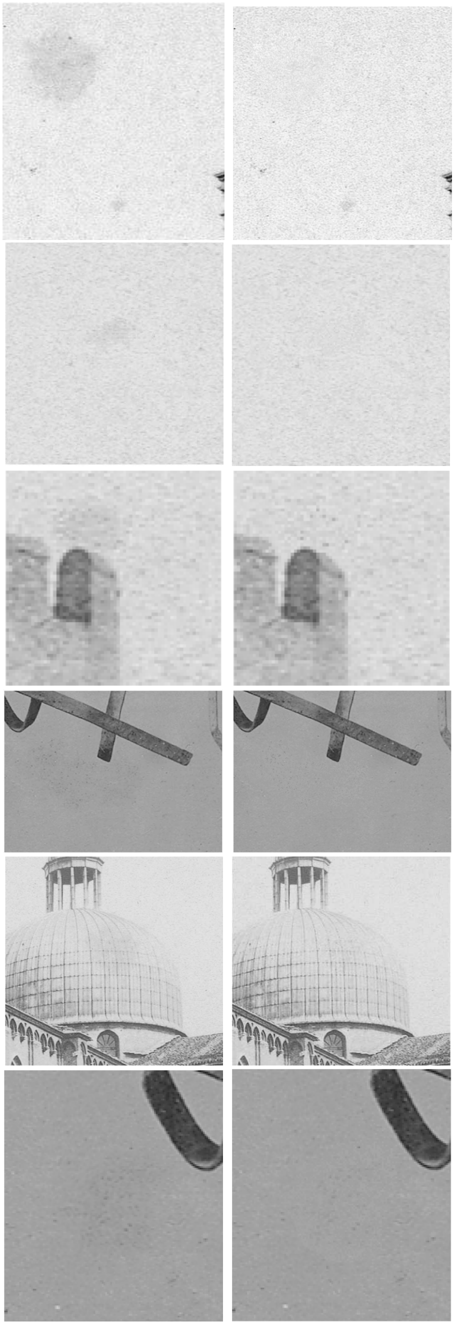

Figure 3: Semi-transparent blotches: Original (*Left*) and restored (*Right*) images.

ages even though it is based on less assumptions about the considered degradation.

All the aforementioned features make the proposed method a valid and promising attempt to the definition of a user's friendly and global restoration framework. Future research will be then oriented to further generalize the proposed restoration framework to make it more flexible and adaptive to a wider class of degradation kinds.

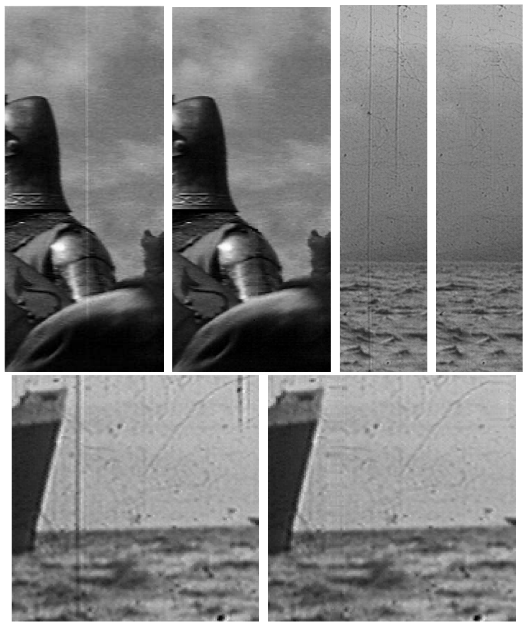

Figure 4: Line-scratches: Original (*left*) and corresponding restored images (*right*).

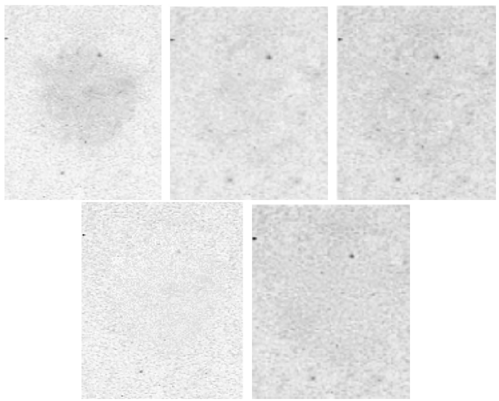

Figure 5: *Clockwise order* Original image, restored using methods in [9, 4, 2], and the proposed one.

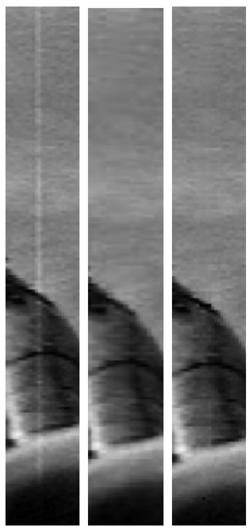

Figure 6: *Left to right* Original image and restored using the methods in [28] and the proposed one.

REFERENCES

[1] V. Bruni, D. Vitulano. A generalized model for scratch detection. IEEE Trans. on Image Proc., Vol. 13, No.1, 44-50, Jan. 2004.

[2] V. Bruni, A. Crawford, A. Kokaram, D. Vitulano, Semi-transparent blotches removal from sepia images exploiting visibility laws, Sig. Image and Video Proc., Springer, 2011.

[3] D. Corrigan, A. Kokaram, Automatic treatment of film tear in degraded archived media. Proc. of ICIP '04, Singapore, Oct. 2004.

[4] A. Greenblatt, S. Agaian, K. Panetta, Restoration of images damaged by semi-transparent water blotches using localized image enhancement, Proc. of SPIE 2008, 2008.

[5] M. Gulu, O. Urhan, S. Erturk, Scratch detection via temporal coherency analysis and removal using edge priority based interpolation, Proc. of IEEE Int. Symp. on Circ. and Syst., 2006, May 2006.

[6] A. Kokaram. On missing data treatment for degraded video and film archives: a survey and a new bayesian approach. IEEE Trans. on Image Proc., Vol 13, No. 3, 397-415, Mar. 2004.

[7] A. Kokaram. Motion Picture Restoration: Digital Algorithms for Artefact Suppression in Degraded Motion Picture Film and Video, Springer Verlag, 1998.

[8] P. van Roosmalen, R. Lagendijk, J. Biemond. Correction of intensity flicker in old film sequences. IEEE Trans. on Circ. and Syst. for Video Tech., Vol. 9, No.7, 1013-1019, 1999.

[9] F. Stanco, L. Tenze, G. Ramponi, Virtual restoration of vintage photographic prints affected by foxing and water blotches, Journal of Electronic Imaging, Vol. 14, No. 4, 2005.

[10] L. Tenze, G. Ramponi, Line scratch removal in vintage film based on an additive/multiplicative model, Proc. of IEEE-EURASIP NSIP-03, Grado, Italy, June 2003.

[11] S. Tilie, I. Bloch, L. Laborelli, Fusion of complementary detectors for improving blotch detection in digitized films, Pattern Recognition Letters, Vol. 28, 1735-1746, May 2007.

[12] T. Vlachos, Flicker Correction for Archived Film Sequences, IEEE Trans. on Circ. and Syst. for Video Tech., Vol. 14, 508-516, Apr. 2004.

[13] S. Agaian, B. Silver, K. Panetta, Transform Coefficient Histogram Based Image Enhancement Algorithms Using Contrast Entropy, IEEE Trans. on Image Proc., Vol. 16, No. 3, Mar. 2007.

[14] H. Sheikh, A. Bovik, Image Information and Visual Quality, IEEE Trans. on Image Proc., Vol. 15, No. 2, Feb. 2006.

[15] Z. Wang, A. Bovik, H. Sheikh, E. Simoncelli, Image quality assessment: From error visibility to structural similarity, IEEE Trans. on Image Proc., Vol. 13, No. 4, 600-612, Apr. 2004.

[16] Z. Wang, Q. Li, Information Content Weighting for Perceptual Image Quality Assessment, IEEE Trans. on Image Proc., Vol. 20, No. 5, 1185-1198, May 2011.

[17] V. Bruni, A. Crawford, A. Kokaram, D. Vitulano, Visual perception of semitransparent blotches: detection and restoration, I-Tech Book: Brain, Vision and AI, chapter 1, 2008.

[18] W. Hoffman, The Lie algebra of visual perception, J. of Math. Psycho., Vol. 3, No. 1, 65-98, Febr. 1966.

[19] P.C Dodwell, The Lie transformation group model of visual perception, Perception and Psychophysics, Vol.34, No. 1, 1-16, 1983.

[20] V. Varadarajan, Lie groups, Lie algebras and their representations, Prentice-Hall Series in Modern Analysis, Englewood Cliffs, N.J., 1974.

[21] S. Helgason, Differential geometry and symmetric spaces, Pure and Appl. Math., Vol. XII. Academic Press, New York-London, 1962.

[22] T. Drummond, R. Cipolla, Application of Lie algebras to visual servoing, Int. J. of Computer Vision, Vol. 37, No. 1, 21-41, 2000.

[23] D. Youla, H. Webb, Image Restoration by the Method of Convex Projections: Part 1 - Theory,IEEE Trans. on Med. Imag., Vol. 1, No. 2, 81 -94, 1982.

[24] S. Winkler, Digital Video Quality. Vision Models and Metrics, Wiley 2005.

[25] R. Gonzalez, R. E. Woods, Digital Image Processing, Prentice Hall, 2nd Edition, 2002.

[26] M. Nilsson, M. Dahl, I. Claesson, The successive mean quantization transform, Proc. of ICASSP, pp. 429-432, 2005.

[27] T. Pappas, R. Safranek, J. Chen, Perceptual criteria for image quality evaluation, Handbook of Image and Video Processing, pp. 939-959, Academic Press, 2005.

[28] V. Bruni, A. Kokaram,D. Vitulano, Fast removal of line scratches in old movies, Proc. of ICPR'04, Vol. 4, pp. 827-830, Aug. 2004.

[29] V. Bruni, E. Rossi, D. Vitulano, Image Restoration via Human Perception and Lie Groups, Proc. of VISAPP 2012, Vol. 1, SciTePress, Feb. 2012.